Journal of Applied Polymer Science

Influence of the Polymer Structure on the Drug–Polymer Interactions in the Micellar Nanoparticles: Mixed Homopolymer and Copolymerized Cores

Salman Hassanzadeh, Sepideh Khoee
Polymer Chemistry Department, School of Chemistry, University of Tehran, P.O. Box 14155-6455, Tehran, Iran
Correspondence to: S. Khoee (E-mail: khoee@khayam.ut.ac.ir)

ABSTRACT: The two strategies of mixing and copolymerizing were used to incorporate more drug-compatible butylene adipate (BA) repeating units into the less drug-compatible unsaturated poly(*cis*-2-butene adipate) (PCBA) core of micelles. Novel parameters were defined on the basis of the hydrodynamic radius of the particles. A comparison of the encapsulation capabilities of the different copolymerized and mixed micelles was performed with these parameters. Both the mixed and core-copolymerized micelles were indicated to have spherical morphologies and synergic properties of the copolymerized and mixed repeating units. They exhibited a higher encapsulation of the drug, a lower critical micelle concentration, and more controlled release behavior compared to the pure PCBA micelles. In addition, a comparative study of the two strategies was performed in the presence of same molar ratios of BA in the core. The mixed micelle formulation was found to be more effective in making a core more compatible to quercetin (as a model anticancer hydrophobic drug) with better pharmaceutical properties. © 2012 Wiley Periodicals, Inc. J. Appl. Polym. Sci. 129: 652–664, 2013

KEYWORDS: copolymers; drug-delivery systems; micelles; nanostructured polymers; polyesters

Received 21 May 2012; accepted 25 August 2012; published online 22 November 2012
DOI: 10.1002/app.38547

INTRODUCTION

With regard to the ability of amphiphilic block copolymers to self-assemble in water into micelles at nanometer scales, scientists have proposed a wide range of potential applications. One promising application of these micelles is in the area of drug-delivery systems.[1–7]

The capacity of micelles to enhance the solubility of hydrophobic and bioactive molecules stems from their unique core–shell structure, where a hydrophilic corona outer shell stabilizes the hydrophobic reservoir inner core. The drug molecules in the core can be incorporated by different interactions, depending on their physicochemical properties. The active and passive targeting, in addition to prolonged *in vivo* circulation times and adequate retention of the drug within the carrier advantages, are achieved by the unique steric structure of the shell and small nanometer scale of the nanoparticles.[2] These features would enhance the biodistribution and bioavailability of poor drugs in biological media (e.g., the body at the site of action), and this provides better pharmacological effects, especially for the therapy of some die-hard cancerlike diseases.

Synthetic block copolymers from biodegradable and biocompatible families [e.g., poly(ethylene glycol) (PEG)–polyester–PEG triblocks] display versatile advantages, such as their ease of incorporating functionalities into polymers, over other candidates.[8] Several important parameters, including the drug-loading capacity, release of drug, size, size distribution, and incorporation of functionalities, have to be considered in the design and preparation of desired polymeric micelles for the optimized delivery of a typical drug.[9,10] Generally, the stability of the micelles is addressed by the critical micelle concentration (cmc) as a thermodynamic value. Additionally, the size and size distribution of the core–shell (micellar) nanoparticles depend on the structure and composition of block copolymers (the copolymer molecular weight, hydrophilic–lypophilic balance, etc.) and micelle preparation method (micelle aggregation number, etc.).[11,12]

The release behavior and loading capacity of typical polymeric micelles are dictated by different factors. These factors include the strength of interactions between the drug and core-forming block (the most important factor), the physical state of the micelle core, the amount of drug loaded, the molecular volume of the drug, the length of the core-forming block, the localization of the drug within the micelle, and so on.[13,14] Thus, to prepare micelles with desired optimized tunable drug capacity, release, size, size distribution, and stability, there is a need to use the

Additional Supporting Information can be found in the online version of this article.

right copolymers with a proper core and shell structure for a specific drug. Most of the selected polymeric micelles often lack one or more of the primary conditions, as discussed, of desired nanomedicines.[12]

In this article, we report the comparative results from two methodologies used to make the core of the micellar nanoparticles more compatible with a candidate drug (quercetin). The used methods were the copolymerization of the monomers and the comicelling of the prepared pure copolymers to create a copolymerized micelle core and mixed micelles (a mix of homopolymers in the core), respectively. The copolymerization strategy was used as a synthetic way to combine the ability of the different chemical moieties to create a synergistic effect on the characteristics of the obtained final product.[15] Jiang et al.[15] used a hydrophobic poly(caprolactone-*co*-lactide) segment because it combined the good drug-encapsulation ability of polycaprolactone and the favorable biodegradability of polylactide. The complicated synthetic schemes and practical complex method on large scales are the drawbacks of copolymerization performed to attain better properties.[16] These issues emerged in the mixing strategy of the prepared polymeric molecules of the different components as an easy and efficient way of combining these different abilities. Mixed micelles manifest synergistic properties, such as increased micellar stability and drug-loading efficiency, that are superior to those of the individual components.[17,18]

One could expect that the comicelling of two miscible copolymers with the same hydrophilic and different hydrophobic parts (a less compatible copolymer together with copolymers more compatible to the drug) would provide mixed micelles that would allow better solubilization of the drug. The increased volume of the lipophilic core of the mixed micelle and enhanced interactions between the drug and core would be effective.[19] Therefore, difunctional/multifunctional copolymer micelles can be distinguished as mixed micelles, where one component equips the core by the defined ability and the other component makes it more compatible to the drug.[20,21]

Quercetin (Scheme 2, shown later) as a flavonoid with anticarcinogenic, antiallergic, and chemopreventive or/and chemotherapeutic properties for prostate cancer was used in this study.[22] As a typical hydrophobic drug, it is incorporated into the hydrophobic core of the micelles in the aqueous medium. Quercetin possesses different rings and hydroxyl groups that interact efficiently with esteric functional groups of the polyesters in the core of the nanoparticles via hydrogen bonding and so on.[14]

cis-2-Butene adipate (CBA) repeating units were chosen as one of the components of the even mixing and copolymerization strategy because of the presence of double bonds. The unsaturated bonds in the main-chain structure enable synthetic chemists to alter the structure of the molecules, adding and introducing other functional groups and crosslinking the core(to create more stable nanoparticles). The choice of butylene adipate (BA) repeating units as the second component with their semisimilar chemical structure to CBA was based on their enhanced compatibility with quercetin and better encapsulation properties in comparison to CBA in the prepared monomethoxy poly(ethylene glycol) (MPEG)–poly(butylene adipate) (PBA)–MPEG and MPEG–poly(*cis*-2-butene adipate) (PCBA)–MPEG micellar nanoparticles. The copolymerized polyesteric core of poly(butylene-*co*-*cis*-2-butene adipate) (PBCBA) was synthesized in predetermined molar ratios similar to the applied mixing ratio of the PBA and PCBA to create the same molar ratio of BA and CBA repeating units in the core. The copolymerized core and the binary mixed core of the nanoparticles were precisely compared to each other to determine the advantages and disadvantages of the two proposed modification strategies. The mixed micelle formulation was found to be more effective for providing a more drug-compatible core. The other advantages of the mixed micelles over the copolymerized micelles included the monomodal narrow size distribution of the micelles, a simpler and more efficient preparation procedure, and more controlled release rates.

EXPERIMENTAL

Material

1,4-Butanediol (purum grade), *cis*-2-butene-1,4-diol (>96% cis), and MPEG [weight-average molecular weight (M_w) = 2000] were obtained from Fluka Chemical Co. (Buchs, Switzerland) and were used as received. Adipoyl chloride, hydroquinone, and quercetin dihydride were also obtained from Fluka. Acetone and pyrene were purchased from Merck Chemical Co. Diethyl ether was purchased from Guandong Guango Chemical Co. (China). All of the chemicals were analytical grade and were used without additional purification. Deionized water was used to prepare the various aqueous solutions.

Synthesis of the Block Copolymers

Two sequential synthetic routes were proposed to produce the primary triblocks. In the first step, acid chloride terminated polyesters were formed. In the second step, MPEGs were attached to the terminal activated esteric chains to form MPEG–polyester–MPEG amphiphiles. All of the polyesteric parts were synthesized via a routine solvent-free polycondensation reaction of adipoyl chloride and glycols (1.05:1 molar ratio to the glycols), with a vacuum applied to remove the released acid. A previously predicted amount of hydroquinone was added as an inhibitor in the case of the unsaturated diols.

The hydrophobe polyesteric segments included copolymers of PBCBA, and homopolymers of PBA and PCBA were prepared in molar ratios of 0:1, 0.25:0.75, 0.5:0.5, 0.75:0.25, and 1:0 of *cis*-2-butene-1,4-diols and 1,4-butandiols monomers with adipoyl chloride in the reaction vessel. The ratios of the monomers were measured, and the monomers were placed in 250-mL, three-necked, round-bottom flask already cooled down to 4°C. Then, a predetermined amount of hydroquinone was added to the mixture, and the reaction started smoothly to release HCl gas. Although HCl gas was continuously removed by vacuum, the temperature gradually increased to 70°C. The synthesis reaction of the polyesteric segment in the first step lasted for 6 h at this temperature to prepare the acid chloride terminated polyesters.

In the second step, the excess amount of MPEG (M_w = 2000) was added to the acid chloride terminated polyesters at the same temperature, and the reaction was kept running for

another other 6 h at a reduced pressure to form an amphiphilic triblock. The final viscous melt was poured into an excess volume (about 40 mL) of cooled diethyl ether to precipitate the white powder of the copolymers. The copolymers were purified from excess MPEG three times by washing with distilled water. The resulting copolymers were filtered off and dried at a reduced temperature for 10 h. Because of the one-pot continuous reaction of the block copolymer preparation, the mean yield of the procedure was around 95% (5% loss in the washing step).

Preparation of the Micellar Nanoparticles

The nanoprecipitation method was chosen as it is one of the most convenient and efficient methods for the preparation of core–shell nanoparticles (micellar nanoparticles or nanometric micelles).[23,24] The drug-loaded micelles were prepared through the nanoprecipitation method described previously with minor modifications.[14] Briefly, 10 mg of the MPEG–polyester–MPEG triblock copolymer and a predetermined amount of quercetin were dissolved in an aliquot of acetone as a miscible solvent. The optimized 10% drug/polymer ratio, which was extracted from the optimization experiments, was applied. The obtained acetone solution was added dropwise to 10 mL of distilled water under moderate stirring at room temperature. Then, the acetone as an organic phase was removed completely under reduced pressure. Finally, to remove the aggregated copolymers, unincorporated drug crystals and other big aggregates, the solution was filtered through a 0.45-μm cellulose acetate syringe filter. The final dispersion was frozen and transferred quickly to the lyophilizer to obtain the fine powder of the quercetin-loaded dried nanoparticles.

Methods

Analysis of the Prepared Block Copolymers. The identification and characterization of the synthesized block copolymers were performed with differential scanning calorimetry (DSC), ^{1}H-NMR, Fourier transform infrared (FTIR) spectroscopy, and gel permeation chromatography (GPC) analysis. The compositions of the copolymers were determined by ^{1}H-NMR at room temperature on a Bruker DRX-500 Avance spectrometer (Billerica, MA, United States) with $CDCl_3$ as the solvent. The FTIR spectra of the copolymers were carried out on a Shimadzu IR-460 instrument. Specimens in the form of powder were placed directly on the crystal on the top of the golden gate.

GPC measurements were performed on an Agilent GPC apparatus (Santa Clara, CA, United States) equipped with a refractive index (RI) detector with tetrahydrofuran as a mobile phase at a flow rate of 1 mL/min at 23°C to characterize the polydispersity index (PDI), number-average molecular weight (M_n), and M_w values of the copolymers. The DSC thermograms of the copolymers were acquired by use of a computer-interfaced calorimeter (PerkinElmer Pyres DSC instrument) under a nitrogen atmosphere and at a heating rate of 10°C/min from ambient to 350°C. The mixed sample of MPEG–PBA–MPEG and MPEG–PCBA–MPEG in the bulk state for DSC analyses were prepared in the same molar ratios as the molar ratios of the copolymerization reaction. The predetermined molar ratios of the copolymers were weighed and melt-blended at 70°C for 1 h. Then, the viscous final melt was poured into cool diethyl ether to get the fine powder of the mixed copolymers. The precipitates were vacuum-dried for 10 h, and this gave the white fine powder of the mixed copolymers.

Nanoparticle Characterizations of the Micellar Nanoparticles. The amounts of the incorporated drug were determined gravimetrically by UV absorption at their maximum wavelength on a Cary 100 biospectrophotometer (Varian INC. Palo Alto, CA, United States). The yield, drug-loading content (DL), and encapsulation efficiency (EE) were obtained by eqs. (1), (2), and (3), respectively:

$$\text{Yield}(\%) = \frac{\text{Weight of the micelles}}{\text{Weight of the feeding polymer and drug}} \times 100 \quad (1)$$

$$\text{DL}(\%) = \frac{\text{Weight of the drug in themicelles}}{\text{Weight of the micelles}} \times 100 \quad (2)$$

$$\text{EE}(\%) = \frac{\text{Weight of the drug in themicelles}}{\text{Weight of the feeding drugs}} \times 100 \quad (3)$$

The polymer micellation efficiency (PME) explains the efficiency of the copolymers that aggregate into micelles:

$$\text{PME}(\%) = \frac{\text{Weight of the polymer in themicelles}}{\text{Weight of the feeding polymer}} \times 100 \quad (4)$$

Dynamic light scattering (DLS) measurements were performed with a Malvern Zetasizer Nano series instrument (Worcestershire, UK) to determine the hydrodynamic radius (R_h) and size distribution. Before the DLS measurements, all of the solutions were filtered through 0.45-μm syringe filters. Morphological examination of the micellar nanoparticles was conducted with transmission electron microscopy (TEM), atomic force microscopy (AFM), and scanning electron microscopy (SEM). For TEM, one drop of a dispersion containing 2 wt % phosphotungstic acid was placed on a copper grid with Formvar film, dried, and negatively stained. The prepared sample was applied to a Philips CM120 TEM instrument at an acceleration voltage of 120 keV to obtain the images. For AFM measurements, all of samples were cast on mica substrates (that were cleaned by layer removal) from a dilute dispersion of the prepared nanoparticles (10^{-7} mg/mL). The films were dried for 2 days in a dust-free chamber at room temperature before AFM observation. Atomic force micrographs were recorded under ambient conditions with silicon cantilever tips (PPP-NCH, 300–330 kHz, 42 N/m from the nanosensors) with an Asylum Research MFP-3D-Bio machine (Santa Barbara, CA) in noncontact mode under ambient conditions. SEM analysis was carried out with a Cambridge S-360 SEM instrument. Before examination, the samples were sputter-coated with gold to render them electrically conductive.

The newly defined parameters were calculated and compared with the experimentally obtained R_h and the presumption of the nanoparticles as free random-coil PEGs. These parameters were considered to be the minimum values. They were used together with the drug loadings to evaluate the encapsulation capability of the cores and to compare the compatibility of the core-forming polymers and quercetin.

A correlation was established between R_h of a single molecular random-coiled PEG and its M_w by the Stokes–Einstein relationship:

$$R_h = k_B T / 6\pi\eta_0 D_0 \quad (5)$$

In Eq. (5) (D_0 is the diffusion constant, η is viscosity, T is temperature and k_B is Boltzmann's constant), with $T = 25°C$ and $\eta_0 = 1$, the analytical expression is given as[25,26]

$$R_h = 0.145 M_w^{0.571} (\text{Å}) \quad (6)$$

By presuming the obtained R_h of the micellar nanoparticle as a free random-coiled hydrated single-molecular PEG, we calculated the theoretical minimum value of M_w of the micelles. The real structure of the micellar nanoparticles was composed of the swollen hydrated shell and the hydrophobic compact cores. With regard to the obtained molecular weight as an aggregate molecular weight of the micelle (AMW) and with the molecular weight of the polymers, the minimum number of aggregation (mN_{agg}) was acquired:

$$mN_{agg} = \text{AMW}/\text{M}_w \quad (7)$$

The number of the polymeric aggregated chains (concentration of polymers in the micelles) and micelles (concentration of the micelles) were also calculated from the weight of the polymer in the micelles (obtained from the PME value) and the total number polymeric aggregated chains and mN_{agg} values. With a known drug-loading value, number of micelles and polymeric aggregated chains provided us with some interesting novel parameters, including the mean number of the drug per particle (DPP) and mean number of the drug per chain (DPC).

$$\text{DPP} = \frac{[\text{Encapsulated drug}]}{[\text{Micelles}]} \quad (8)$$

$$\text{DPC}_{\text{feed}} = \frac{[\text{Feed drug}]}{[\text{Feed polymers}]} \quad (9)$$

$$\text{DPC}_{\text{micelles}} = \frac{[\text{Encapsulated drug}]}{[\text{Polymers in the micelles}]} \quad (10)$$

Because of the similar feed drug/copolymer weight ratios (10% w/w) and the different molecular weights of the copolymers, different feed DPCs were applied primarily. As a comparable factor for micelles, the micelle encapsulation efficiency (MEE) was introduced. Dividing the DPC in the micelles by the feed DPC provided us with a quantity indicating the capability of the different core compositions to make maximum interactions and, in turn, the maximum encapsulation of the feed drug:

$$\text{MEE} = \frac{\text{DPC}_{\text{micelles}}}{\text{DPC}_{\text{feed}}} \quad (11)$$

Subtracting the already known molecular weight of the hydrophilic parts from that of the triblock, we determined the molecular weight of the hydrophobic polyesteric segment. Dividing this value by the repeating unit molecular weight, we acquired the mean number of esteric functions per chain and particles. Then, the mean number of functions per drug (FPD) as another valuable parameter were calculated with Eq. (12):

$$\text{FPD} = \frac{[\text{Functions in the nanoparticles}]}{[\text{Encapsulated drug}]} \quad (12)$$

The FPD, the MEE together with the drug-loading values, provided worthy information about the extent of the interactions between the different copolymers and quercetin.

The cumulative *in vitro* release of quercetin from the nanoparticles was evaluated with a 12-kDa dialysis bag by the diffusion technique. All of the details and methods were described previously in detail.[14] Two theoretical models were performed for the mechanistic interpretations of the cumulative released drug from the nanoparticles as a bulk degrading sphere system. The Higuchi model considers the drug release from the polymeric matrix just through a diffusion process on the basis of Fick's law [Eq. (13)]:

$$\frac{M_t}{M_\infty} = kt^{1/2} \quad (13)$$

where the constant k reflects the formulation characteristics and M_t and M_∞ are the amounts of released drug at time t and infinity, respectively. The second model is the Korsmeyer–Peppas or Power law model. The power law as a general equation describes various mechanisms of transportation [Eq. (14)]:

$$\frac{M_t}{M_\infty} = k' t^n \quad (14)$$

where k' is a constant incorporating the geometrical and structural characteristics of a system and n is an exponent of release (characterizing the mechanisms). For the first 60% of the fractional release of spheres, Fickian diffusion is the dominant mechanism when $n < 0.43$. The anomalous mechanism is the main mechanism when $0.43 < n < 1$, and finally, the zero-order release mechanism is dominant when $n = 1$.

Fluorimetric measurements of the prepared micelles used to determine cmc were recorded on a PerkinElmer LS50B luminescence spectroscope with pyrene as a hydrophobic fluorescent probe. The method was previously reported in detail.[27] The synergism of the triblock mixing could led to the forecasted cmc's of the mixed micelles. In the case of the ideal mixing of the amphiphiles, the phase separation model could be used to calculate cmc of the mixture [Eq. (15)]:[28]

$$\frac{1}{\text{cmc}_{\text{mix}}} = \frac{\alpha_{\text{PBA}}}{\text{cmc}_{\text{PBA}}} + \frac{\alpha_{\text{PCBA}}}{\text{cmc}_{\text{PCBA}}} \quad (15)$$

where cmc_{PBA} and cmc_{PCBA} refer to the critical micelle concentration values of the pure PBA and PCBA copolymers, respectively, and α_{PBA} and α_{PCBA} are the respective molar fractions of the copolymers in the mixture.

Statistical Analysis. All particle diameters, EEs, and releases data were collected in triplicate. The data are represented as the mean plus or minus the standard deviation (SD). The data were analyzed with the T test, and the statistical significance was set at $p < 0.05$.

RESULTS AND DISCUSSION

Several factors influence the encapsulation of a hydrophobic drug. Among them, the compatibility of the drug and the hydrophobic core are the major factors.[29] The physical sense of

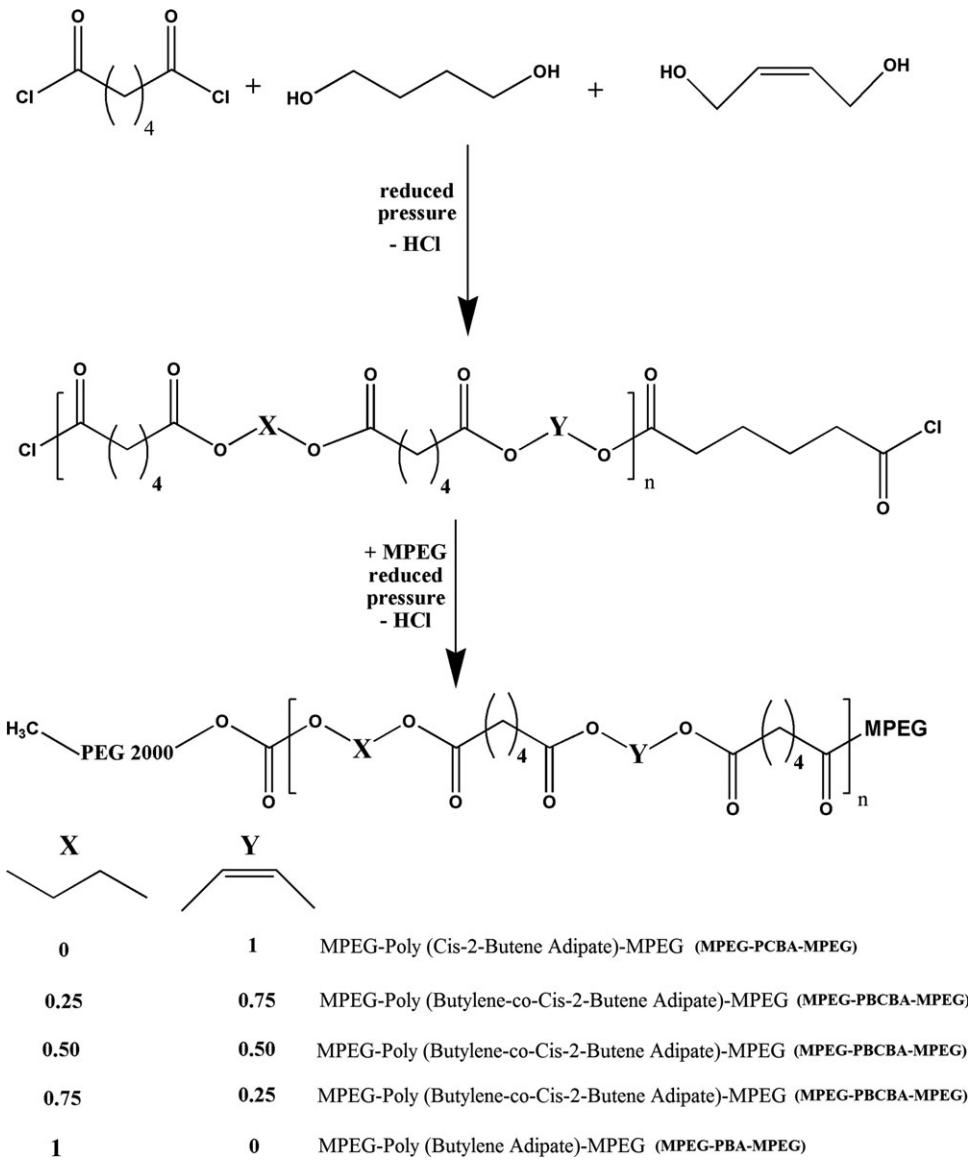

X	Y	
0	1	MPEG-Poly (Cis-2-Butene Adipate)-MPEG **(MPEG-PCBA-MPEG)**
0.25	0.75	MPEG-Poly (Butylene-co-Cis-2-Butene Adipate)-MPEG **(MPEG-PBCBA-MPEG)**
0.50	0.50	MPEG-Poly (Butylene-co-Cis-2-Butene Adipate)-MPEG **(MPEG-PBCBA-MPEG)**
0.75	0.25	MPEG-Poly (Butylene-co-Cis-2-Butene Adipate)-MPEG **(MPEG-PBCBA-MPEG)**
1	0	MPEG-Poly (Butylene Adipate)-MPEG **(MPEG-PBA-MPEG)**

Scheme 1. Chemical synthesis routes for the MPEG–PBCA–MPEG, MPEG–PBCBA–MPEG, and MPEG–PBA–MPEG triblock copolymers.

the drug–polymer compatibility is the enhanced interaction of the polymer and the drug in the core, which leads to a higher drug encapsulation.[30,31]

To achieve this goal, mixtures of 1,4-butanediol and *cis*-2-butene-1,4-diol in molar ratios of 0:1, 0.25:0.75, 0.5:0.5, 0.75:0.25, and 1:0 were used to provide single homopolymers and random copolymers as hydrophobic segments of polymeric carriers. For the preparation of the amphiphilic copolymers, a two-step polycondensation reaction was planned. The acid chloride terminated polyester was prepared from the first step followed by the reaction with an excess amount of MPEG in the second step to produce different triblock copolymers (Scheme 1). The structures of the prepared triblocks were confirmed by FTIR and ^{1}H-NMR spectroscopy (see Supporting Information).

The M_n, M_w, and melting temperature (T_m) values of the different triblock copolymers are given in Table I. All of the copolymers showed a unimodal peak in GPC; this implied that the polycondensation reactions were carried out effectively. The chemical structures of the PBCBAs were analyzed by their ^{1}H-NMR integral peaks to obtain the 1,4-Butanediol /cis-2-butene-1,4-diol (BD/CBD) ratio in the copolymerized polymer. The obtained values were in good agreement with the feeding ratio with normal minor differences.

DSC thermograms of the MPEG–PBA–MPEG and MPEG–PCBA–MPEG copolymers showed the presence of a shoulder near the single sharp melting point peak [Figure 1(a), Table I]. The resulting triblock copolymers were proven to be semicrystalline with T_m's of 54.97°C for MPEG–PBA–MPEG and 59.3°C for MPEG–PCBA–MPEG. It was obvious that the presence of MPEG (MPEG 2000 T_m = 50°C) influenced the crystallinity of the polyesteric blocks because of mutual effects. The melting points of the pure PBA and PCBA were reported to be 60 and 62°C, respectively.[14,32,33] The crystallized MPEG phase peak was

Table I. Major Characteristics of the Synthesized Block Copolymers

Triblock copolymer of	BD/CBD[a]	BD/CBD[b]	M_n[c]	M_w[c]	M_w/M_n[c]	T_m (°C)[d]
PCBA	0/100	0/100	6198	11,469	1.85	59.3
PBCBA25	25/75	26/74	4161	9,507	2.28	46.2
PBCBA50	50/50	50/50	4642	8,971	1.93	51.9
PBCBA75	75/25	77/23	7100	11,058	1.56	50.3
PBA	100/0	100/0	7577	13,103	1.73	54.9

[a]Feed ratio of 1,4-butanediol to *cis*-2-butene-1,4-diol.
[b]Polymerized ratio of 1,4-butanediol to *cis*-2-butene-1,4-diol measured by ^{1}H-NMR.
[c]Measured by GPC.
[d]Measured by DSC.

present as a small shoulder for the PBA and PCBA triblock peaks. The shift of the melting peaks to lower temperatures in the different compositions of the PBCBA triblock copolymers indicated that the mobility of the polyesteric cores increased because of the decrease in the stereoregularity and the crystallization of this block [Figure 1(a)].

To compare the physical properties of the previously synthesized copolymers with their corresponding mixed homopolymers, two-component molten mixtures were prepared. The DSC thermograms showed a single T_m peak for the PBA/PCBA triblock blends at 55.9, 55.0, and 55.7°C for mixed triblocks with 25, 50, and 75 mol % 1,4-butanediol, respectively [Figure 1(b)]. The presence of the T_m peaks between those of the parent polymers revealed that they were miscible polymer blends.

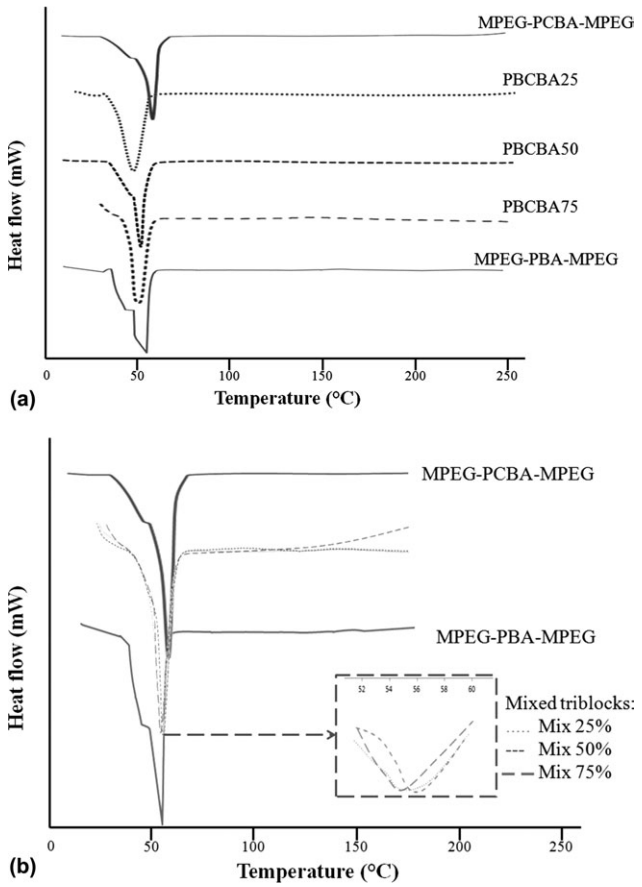

Figure 1. DSC curves of (a) MPEG–PBA–MPEG, MPEG–PCBA–MPEG, and the three prepared random copolymerized MPEG–PBCBA–MPEG triblocks and (b) MPEG–PBA–MPEG, MPEG–PCBA–MPEG, and the mixed triblock copolymers.

By comparing the FTIR spectra of free quercetin (Scheme 2) against those of the empty triblock copolymer and the quercetin-loaded triblock copolymer (Figure 2a), we demonstrated that the molecular dissolution of the drug into the nanoparticle core led to a significant decrease in the intensity of the hydroxyl absorption at 3200–3570 cm^{-1}. This peak corresponded to the hydrogen-bonded OH in the pure crystallized quercetin. The molecular dispersion of quercetin within the polymeric matrix in the core was emphasized by the absence of an endothermic quercetin melting-point peak at 226.2°C in the DSC curve of the quercetin-loaded PCBA micelles [Figure 2(b)].[34] It is noteworthy that the quercetin-loaded triblock copolymer showed a slightly lower melting point than the empty one (micelle T_m = 52.95°C). This could have been related to the plasticizer effect of the entrapped drug in the core of the micelles.

On the other hand, the presence of a broad and weak OH absorption of the quercetin-loaded PBA at 3200–3570 cm^{-1} (in the FTIR spectra) confirmed the presence of hydrogen bonding between the hydroxyl groups of quercetin and the polyesteric core.

Micellar nanoparticles were prepared by a nanoprecipitation method from mixed, single, and cotriblock copolymers. The drug loadings, EEs, particle sizes, and size distributions of the different mixed, single, and cotriblock copolymers were measured (Table II). EE decreased significantly from 87.09 to 24.23% when the saturated diol was changed to an unsaturated

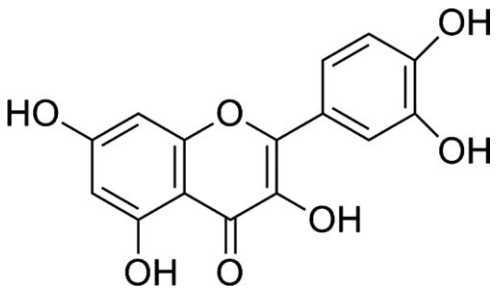

Scheme 2. Chemical structure of quercetin.

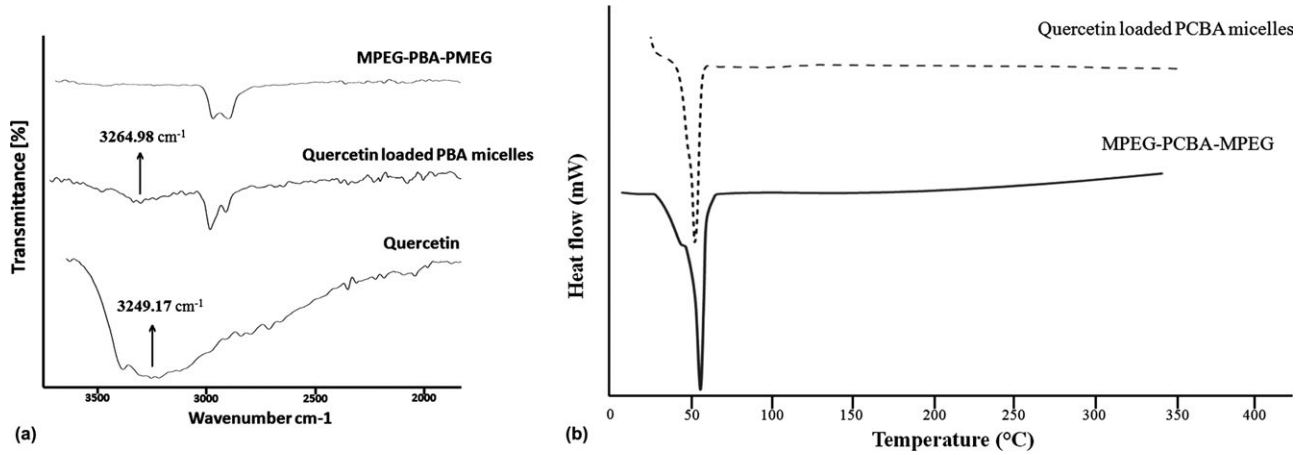

Figure 2. (a) FTIR spectrum and (b) DSC curve of the quercetin-loaded and empty triblock copolymers.

one in the hydrophobic part of the amphiphilic copolymers. A similar decrease in the drug loading from 12.08 to 3.46% was also observed, whereas no remarkable change in the micelle size was found. These results imply that contrary to our expectations, carbon–carbon double bonds as a new functionality did not lead to an increase in the degree of interaction between quercetin and the polyesteric core. To manipulate the functionalities in PCBA (unsaturated bonds in the core), there was a need to modify the core to have more efficient encapsulating particles.

As reported before,[14] the main interaction of quercetin in the polyesteric core of the micelles was hydrogen bonding between its hydroxyl group and its esteric functions. Also, the reported studies on hydrogen-bonded systems emphasized that the geometry and direction of the donor–acceptor functional groups were very important in the creation of strong directional hydrogen bonding.[35] Mixing and copolymerization are the two main methods existing for the introduction of saturated units into the structure of an unsaturated polyesteric core to enhance the aforementioned interactions. According to Table II, we found that the drug-loading and EE values of all of the modified copolymers increased. However, this increment was higher for mixed copolymers than cocopolymers with similar compositions.

The diameters of the micellar nanoparticles were under the control of the polymer composition and structure and ranged from 66 to 104 nm. The R_h values in the copolymerized and mixed micelles increased in comparison to those of the single copolymer micelles. The results illustrate that micelles with more compact internal structures were produced from a single copolymer in the PBA and PCBA samples. This means that the single copolymers' higher tendency to crystallize led to a higher regularity in their core structure. This conclusion was in good agreement with our previous DSC data.

Because of the varied pharmacokinetic properties of different size populations, a broad size distribution is an undesirable property for micellar nanoparticles in drug-delivery applications.[12] The PDIs of the modified cores were acceptably between 0.101 and 0.251. However, the significant decrease in the PDI in the mixed micelles indicated that only one population of mixed micelles was formed by the complete comicellation of the mixed triblocks.

Thermodynamically stable micelles were formed at concentrations above their cmc.[12] The cmc value was influenced by the hydrophilic–lypophilic balance parameter of the amphiphilic molecules.[36] Because the hydrophilic parts in the prepared block copolymers were similar, the cmc values were greatly influenced

Table II. Physicochemical Properties of the Quercetin-Loaded Polymeric Micelles

Sample	Drug loading (%)[a]	EE (%)	PME	Yield (%)	R_h (nm)	PDI	cmc[c]
PBA	12.08 ± 0.3	87.09 ± 2.3	63.38	65.54	33.26 ± 2.1	0.111	1.74×10^{-6}
PCBA	3.46 ± 0.2	24.23 ± 1.4	67.25	63.68	34.66 ± 2.5	0.129	3.12×10^{-6}
PBCBA25	4.81 ± 0.2	37.99 ± 1.8	75.20	71.82	45.21 ± 3.7	0.141	2.40×10^{-6}
PBCBA50	5.97 ± 0.1	59.11 ± 1.6	93.10	90.01	49.44 ± 3.3	0.242	2.11×10^{-6}
PBCBA75	8.53 ± 0.2	76.36 ± 2.1	76.43	76.42	44.02 ± 2.9	0.251	1.47×10^{-6}
Mix 25%	7.26 ± 0.2	58.08 ± 2.0	74.20	72.73	47.01 ± 3.6	0.101	2.64×10^{-6}
Mix 50%	9.82 ± 0.4	79.54 ± 3.3	73.10	73.64	50.1 ± 2.7	0.133	2.23×10^{-6}
Mix 75%	11.84 ± 0.3	93.23 ± 2.5	69.42	71.58	51.6 ± 3.2	0.143	1.96×10^{-6}

[a]The drug-to-copolymer ratio in the feed was optimized at 10 wt %.
[c]Calculated from fluorescence analysis.

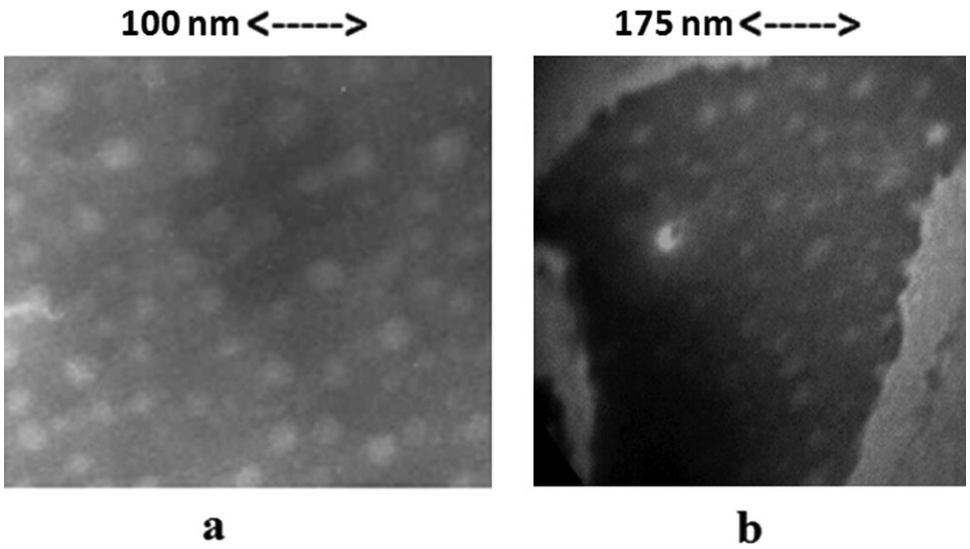

a
b

Figure 3. TEM micrographs of the quercetin-loaded micelles: (a) PBA and (b) mix 50%.

by the hydrophobicity and composition of hydrophobic domains.[37] The cmc values of samples were measured by a fluorometric method. The phase separation equation [Eq. (14)] was used to calculate the cmc values of the mixed micelles. The calculated cmc's for the copolymers in this regime indicated good stability with low values for all of the micelles; this is typical for amphiphilic block copolymers. With the hydrophobic segments of the PBA and PCBA copolymers, it seemed that the greater PBA hydrophobicity caused the lower cmc. The incorporation of more hydrophobic BA repeating units in the core of the modified micelles by both the copolymerization and mixing methods led to the more stable micelles and lower cmc's in comparison to those of PCBA.

To investigate the morphology of the micelles, different microscopic techniques were conducted, including TEM, AFM, and SEM. Figure 3 shows the TEM micrographs of the typical quercetin-loaded PBA [Figure 3(a)] and mixed 50% micelles [Figure 3(b)]. The TEM micrograph of PBA successfully displays a spherical shape and fine round particles [Figure 3(a)], whereas that of the mixed copolymer exhibits a similar morphology with minor deformation. Figure 4 presents typical SEM micrographs of the PBCBA50 (nanoparticles with copolyesteric core with ratio of 50:50 of BA to CBA repeating units) a three scales. Interestingly; a spherical morphology is the characteristic of this modified cocopolymer, too. The AFM images of the quercetin-loaded mixed micelle (mix 50%) exhibits a particle shape

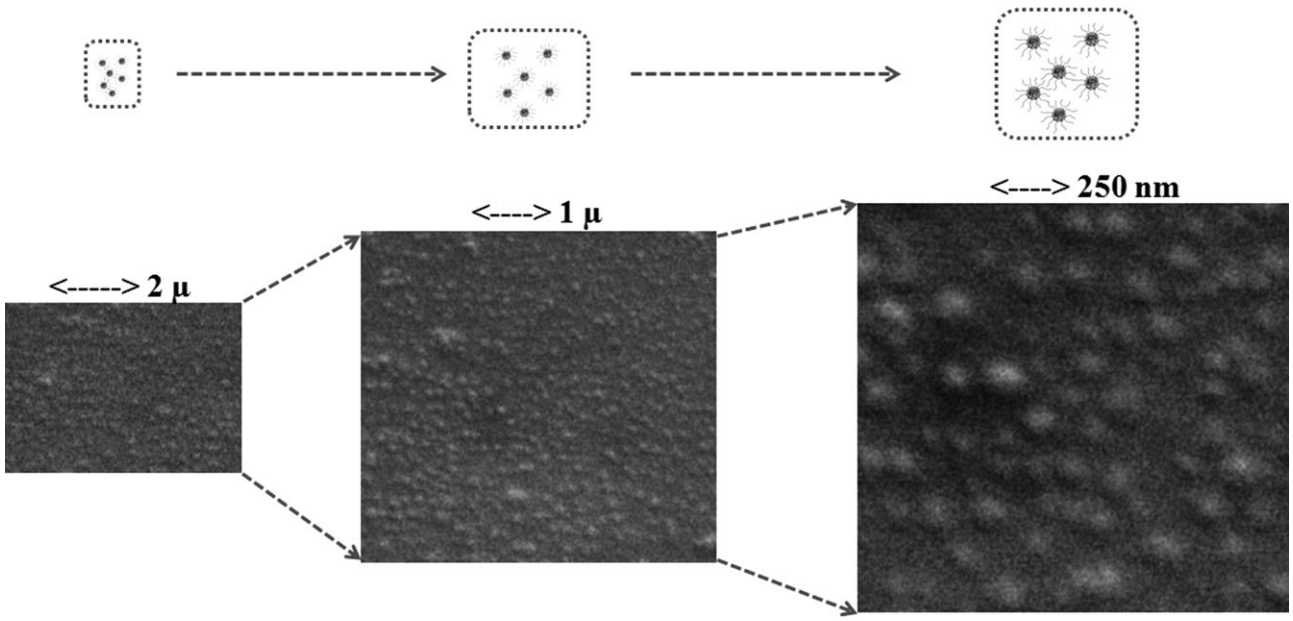

Figure 4. SEM micrographs of the quercetin-loaded PBCBA50 at three scales.

Applied Polymer SCIENCE

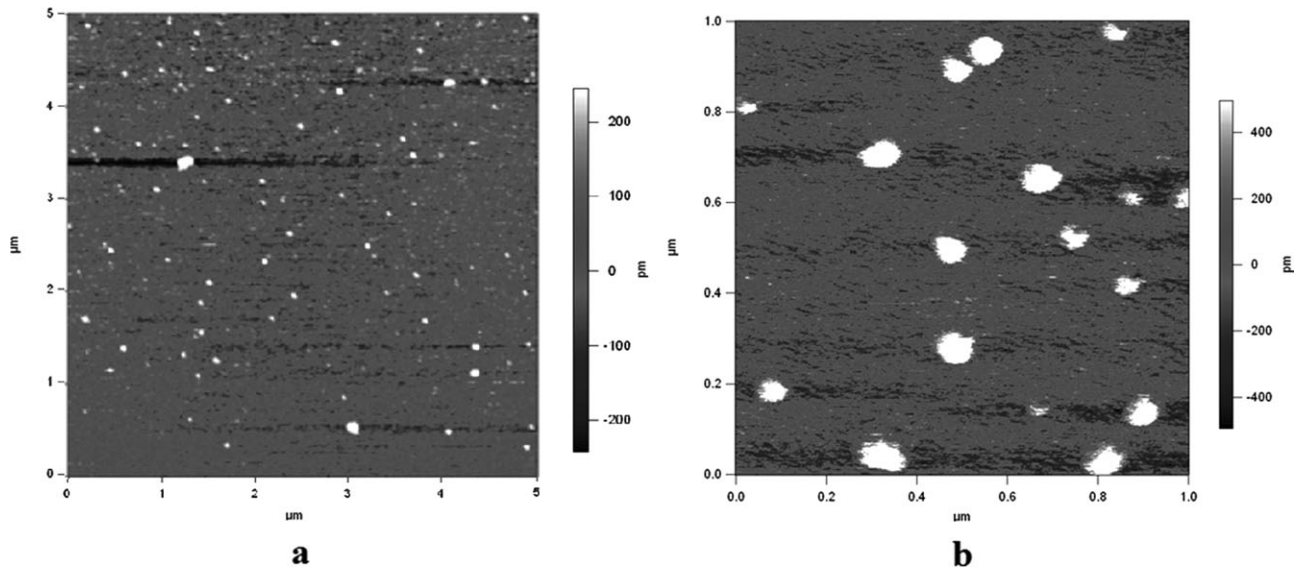

Figure 5. AFM images of the quercetin-loaded mix 50% micelles: (a) 5 and (b) 1 μm.

similar to that of TEM micrographs with a difference in sizes (Figure 5). Because of the negative staining of the dispersions by hydrophilic staining, the mean radius of the hydrophobic core (R_{core}) was visible through TEM, whereas in AFM and SEM, the whole radius of the micelle ($R_{particle}$) was visible ($R_{particle} = R_{core} + R_{shell}$) (Rshell is radius of the shell).

The presence of monodisperse particles in the TEM and AFM images of the mixed micelles and a narrow unimodal peak in the DLS curve (Figure 6) were evidence of a good comicellization of the two single copolymers (i.e., PCBA and PBA) during the preparation.

The same morphologies and preparation conditions for the micelles implied that the chemical composition of the copolymers in the core was the key factor in the control of the drug loading, EE values, and quercetin–polyester affinity. By assuming the actual micellar particle as a free random-coil hydrated PEG, we could then quantify the number of aggregation (N_{agg}), DPP, MEE, and FPD parameters in their minimum values for the micelles.

The results in Table III illustrate the increases in N_{agg} of the copolymerized and mixed micelles in comparison to their single copolymers (PBA and PCBA). These results coincided with our previous observations, in which the particle size of the single copolymers was smaller than those of the mixed and copolymerized ones. The DPP values depend on the amount of encapsulated quercetin and the number of micelles (affected by cmc, N_{agg}, and PME values). Despite the same drug/polymer ratios (10% w/w), different feed DPCs (number of drug molecules per chain of copolymer) were recorded; this was due to the difference in the molecular weights of the copolymers in the feed. MEE as a criteria parameter was obtained by the division of DPC in the prepared micelles by DPC in the feed. The higher total interactions led to a greater encapsulation of the drug and a higher ratio of DPC in the micelle to the DPC in the feed. MEE values in agreement with the drug loadings were developed by both the copolymerization and mixing of the PBCA core with more drug-compatible BA repeating units. The results evidenced that the mixed micelles in comparison to the copolymerized micelles could provide better conditions for the encapsulation of greater amounts of the drug.

A similar trend was recognized for FPD. The FPD value provides the proportion of esteric functions population for every single encapsulated quercetin molecule. The FPD value is determined directly by the capability of the different polyesters to prepare optimum conditions and form as many hydrogen bonds as possible. The lower FPD is, the higher the ratio of the drug to esteric functions will be. This means that a lower number of esteric functions could encapsulate one drug molecule by more efficient interactions. In agreement with the dug loadings and MEEs, the interactions between the esteric functions of PCBA could be more efficient via both the copolymerization and mixing modifications with BA repeating units. Lower FPD values for the mixed micelles in comparison to those of the copolymerized ones emphasized the greater efficiency of the mixing strategy. This observation was made despite two facts: (1) there was the same molar ratio of BA repeating units in both the copolymerized core and the mixed micelles, and (2) a favorably decreased crystallinity in the copolymerized core was present

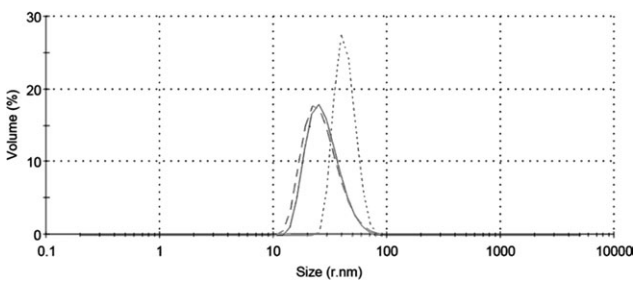

Figure 6. Size measurement of the quercetin-loaded (– – –) PBA, (—) PCBA, and (- - -) 25% mixed micelles.

Table III. Minimum Parameters on the Basis of the Assumption that the Micelle's R_h Was Equivalent to the R_h of Free-Random-Coil PEG

Sample	N_{agg}	DPP	$DPC_{micelles}$	DPC_{feed}	MEE	FPD
PBA	59	352	5.966	4.337	1.3753	15.42
PCBA	72	98	1.361	3.798	0.3583	55.10
PBCBA25	138	219	1.590	3.480	0.4569	34.89
PBCBA50	171	322	1.886	2.971	0.6349	26.49
PBCBA75	113	386	3.658	3.662	0.9991	19.34
Mix 25%	119	366	3.080	3.933	0.7830	25.77
Mix 50%	128	567	4.430	4.068	1.0889	18.80
Mix 75%	131	737	5.646	4.203	1.3432	15.44

(this resulted in a less compact core for dissolving the drug). The similarity of the cmc values for both of the copolymerized and mixed micelles implied that they had no substantial impact on this result. Apparently, the CBA units of PCBA scrambled the required geometrical arrangements of the functional groups for optimal hydrogen bonding with quercetin, whereas that was not the case for BA in the PBA. This fact was manifested by the amount of encapsulated drug. In the copolymerized micelles, it seemed that the random presence of CBA repeating units all over the core-forming copolyester caused part of its weakness to

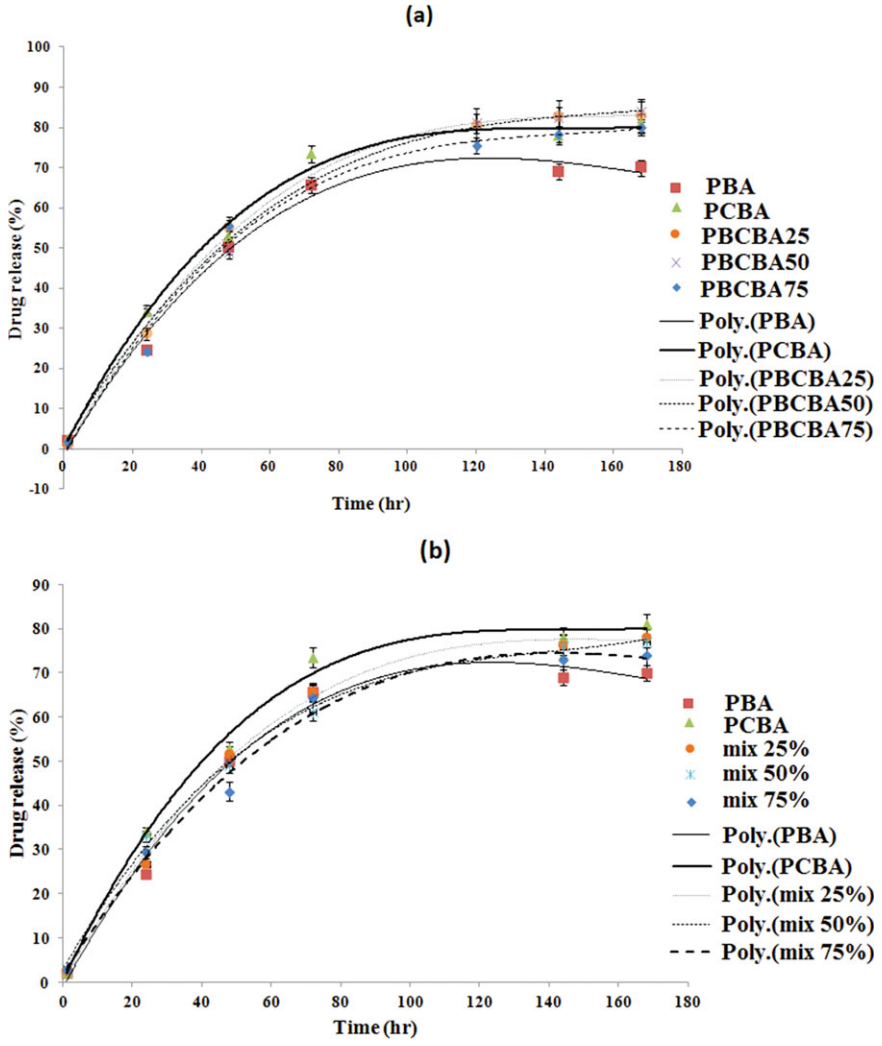

Figure 7. *In vitro* release profiles of the (a) quercetin-loaded copolymerized micelles and (b) mixed micelles ($n = 3$). [Color figure can be viewed in the online issue, which is available at wileyonlinelibrary.com.]

Table IV. Parameters of the Higuchi and Korsmeyer–Peppas Models

		Higuchi		Korsmeyer–Peppas			
Entry	Sample	K	r^2	k'	r^2	n	Release mechanism
1	PBA	5.91067	0.8985	0.3148	0.9982	0.80573	Anomalous
2	PCBA	6.56329	0.9018	0.6455	0.9624	0.71059	Anomalous
3	PBCBA25	7.18027	0.9714	0.1081	0.9990	0.90044	Anomalous
4	PBCBA50	7.11916	0.9848	0.0944	0.9928	0.90651	Anomalous
5	PBCBA75	6.85497	0.9600	0.2286	0.9960	0.81820	Anomalous
6	Mix 25%	6.53024	0.9472	0.3319	0.9914	0.77390	Anomalous
7	Mix 50%	6.24297	0.9710	0.5116	0.9978	0.70097	Anomalous
8	Mix 75%	6.14723	0.9518	0.4611	0.9985	0.71618	Anomalous

make optimal hydrogen bonding to the neighbor BA repeating units. However, in the core of the mixed micelles, a pure polyesteric microcrystalline areas existed that were between the amorphous blend parts. The microstructures with the BA neighborhood reduced the side effects of CBA on the BA units to create optimal interactions with drug.

The *in vitro* release profiles of the copolymerized and mixed nanoparticles are presented in Figure 7(a,b), respectively. The evaluation of the *in vitro* release profiles demonstrated that the composition of the core not only affected the drug loadings but also changed the release trends of the micellar nanoparticles. It was seen that the strong polymer–drug interactions in PBA caused a decreased release rate in comparison to that of PCBA. The release profiles illustrated in Figure 7(a) emphasized that the greater the molar ratio of compatible BA repeating units to quercetin in the copolymerized core was, the slower drug release was. The cumulative release behavior of PCBA was also modified to more controllable kinetic by the preparation of the mixed micelles with PBA. There was a need to look at the release mechanisms of the micelles to interpret it precisely.

The mechanistic studies of the released quercetin were conducted with the Higuchi and Korsmeyer–Peppas models. The k, k', and n parameters of the models were subtracted by linear regression analysis with Microsoft Excel 2007 (Table IV). The fitting accuracy of the models was examined by the correlation coefficient (r^2; in Table IV).

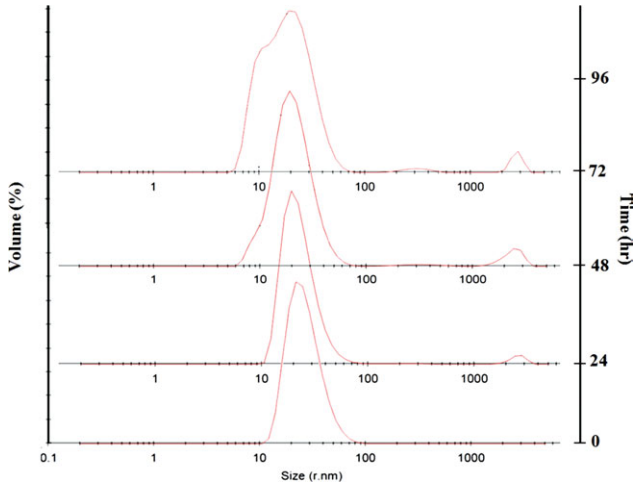

Figure 8. Time-dependent size measurement of the PBA quercetin-loaded micelles. [Color figure can be viewed in the online issue, which is available at wileyonlinelibrary.com.]

Between two drug-release kinetic models, the Korsmeyer–Peppas model was the one that best fit all of the release data (better fitting accuracy). As the obtained n values were between 0.43 and 1, an anomalous release mechanism was found for all of the micelles. In these cases, the mechanisms of release consisted of a mixture of diffusion and swelling. Typically, in biodegradable polymeric micelles, the swelling process is accompanied with events such as the penetration of water, the dissociation of micelles, and the degradation of polymers. A time-dependent size evolution study of the micelle solution with a 1 mg/mL PBA concentration was conducted to investigate the effects of the buffer solution on the degradation of the polymeric micelles (Figure 8). The drug-loaded micelles displayed size changes via surface degradation and dissociation of the micelles that produced larger and smaller particles, respectively (because of coagulation and a chain-detachment effect).

The results in Figure 8 confirm the aforementioned anomalous mechanism, in which a micelle dissociation mechanism cooperated with the diffusion mechanism in the drug-release processes. In Scheme 3, the obtained results are schematically represented.

CONCLUSIONS

In an attempt to make the core of the unsaturated functionalized micelles more compatible with quercetin as a drug, mixing and copolymerizing strategies were used. The binary mixtures of the prepared MPEG–PCBA–MPEG and MPEG–PBA–MPEG were compared to the copolymerized core triblock MPEG–PBCBA–MPEG in the same ratios to attain comparative data. Such structures were efficiently screened in terms of structural characterization, encapsulation capacity, and drug-release profile of the inner core. The obtained micellar nanoparticles were characterized with the synergic properties of the copolymerized and mixed repeating units. Both the copolymerized and mixed micelles exhibited higher encapsulations of the drug, stability of the micelles (lower cmc), and more controlled release trends in comparison to the pure PCBA micelles.

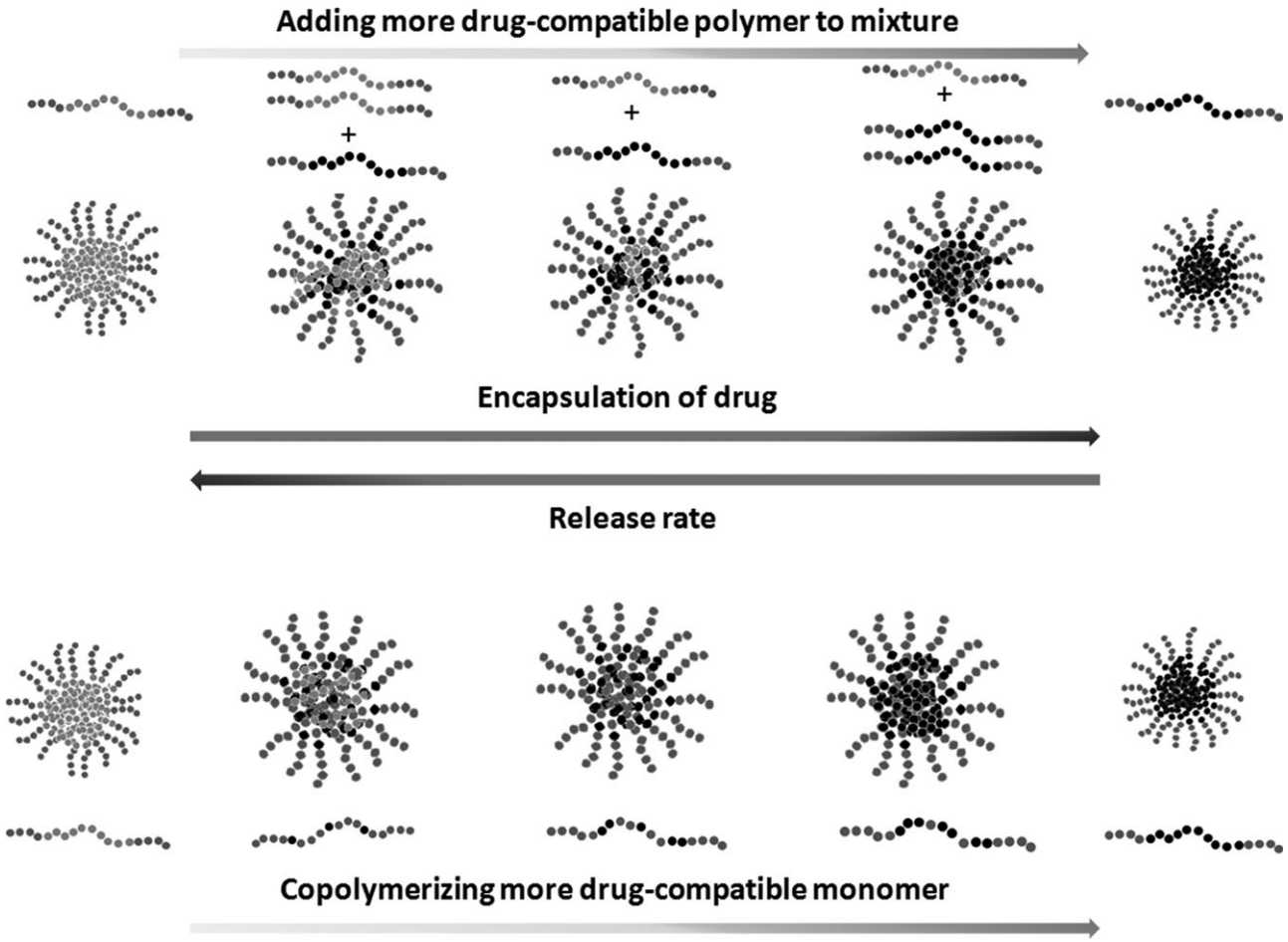

Scheme 3. Representation of the results.

The mixed micelles composed of a PCBA and PBA mixed inner core exhibited noticeable advantages over those with a copolymerized core; these included the following:

1. A monomodal, narrow size distribution of the mixed micelles compared to the relatively wide size distributions of the prepared copolymerized micelles.
2. A higher drug-loading capacity in comparison to the copolymerized micelles at the same molar ratio of the second part. 3. The simpler and more efficient synthetic routes for the modification of the PBCA micelles.
4. The more controlled release rates of the mixed micelles in the first hours.

This study not only provided an indication of the efficiency of the mixing strategy but also emphasized the privileges of the mixing strategy over the copolymerization strategy for the modification of the micellar nanobiomaterials used for drug-delivery systems.

ACKNOWLEDGMENT

The authors wish to express their special gratitude to Patrick Stals at the Chemistry and Chemical Engineering Faculty, Technology University of Eindhoven, for obtaining the AFM micrographs. The authors also thank Seyed Mohammad Hadi Hashemi at the Laboratory of Electron Microscopy of the University College of Science, University of Tehran, for obtaining the TEM micrographs.

REFERENCES

1. Zweers, M. L. T.; Engbers, G. H. M.; Grijpma, D. W.; Feijen, J. J. *Controlled Release* **2006**, *114*, 317.
2. Gaucher, G.; Dufresne, M. H.; Sant, V. P.; Kang, N.; Maysinger, D.; Leroux, J. C. J. *Controlled Release* **2005**, *109*, 169.
3. Hans, M. L.; Lowman, A. M. *Curr. Opin. Solid State Mater. Sci.* **2002**, *6*, 319.
4. Kakizawa, Y.; Kataoka, K. *Langmuir* **2002**, *18*, 4539.
5. Kataoka, K.; Harada, A.; Nagasaki, Y. *Adv. Drug Delivery Rev.* **2001**, *47*, 113.
6. Nishiyama, N.; Kataoka, K. Polym. Ther. *II* **2006**, *193*, 67.
7. Otsuka, H.; Nagasaki, Y.; Kataoka, K. *Adv. Drug Delivery Rev.* **2003**, *55*, 403.
8. Gérard, R. *Prog. Polym. Sci.* **2003**, *28*, 1107.
9. Masayuki, Y.; Mizue, M.; Noriko, Y.; Teruo, O.; Yasuhisa, S.; Kazunori, K.; Shohei, I. J. *Controlled Release* **1990**, *11*, 269.
10. Jiang, W.; Kim, B. Y. S.; Rutka, J. T.; Chan, W. C. W. Expert Opin. *Drug Delivery* **2007**, *4*, 621.

11. Sun, T.-M.; Du, J.-Z.; Yan, L.-F.; Mao, H.-Q.; Wang, J. *Biomaterials* **2008**, *29*, 4348.
12. Ebrahim Attia, A. B.; Ong, Z. Y.; Hedrick, J. L.; Lee, P. P.; Ee, P. L. R.; Hammond, P. T.; Yang, Y.-Y. *Curr. Opin. Colloid Interface Sci.* **2011**, *16*, 182.
13. Allen, C.; Maysinger, D.; Eisenberg, A. Colloids Surf. *B* **1999**, *16*, 3.
14. Khoee, S.; Hassanzadeh, S.; Goliaie, B. *Nanotechnology* **2007**, *18*, 175602.
15. Zhang, L.; Hu, Y.; Jiang, X.; Yang, C.; Lu, W.; Yang, Y. H. J. *Controlled Release* **2004**, *96*, 135.
16. Lasic, D. D. *Nature* **1992**, *355*, 279.
17. Li, L.; Tan, Y. B. *J. Colloid Interface Sci.* **2008**, *317*, 326.
18. Yoo, S. I.; Sohn, B.-H.; Zin, W.-C.; Jung, J. C.; Park, C. *Macromolecules* **2007**, *40*, 8323.
19. Hwang, M. J.; Suh, J. M.; Bae, Y. H.; Kim, S. W.; Jeong, B. *Biomacromolecules* **2005**, *6*, 885.
20. Wang, Y.; Yu, L.; Han, L.; Sha, X.; Fang, X. *Int. J. Pharm.* **2007**, *337*, 63.
21. Lee, E. S.; Gao, Z.; Kim, D.; Park, K.; Kwon, I. C.; Bae, Y. H. J. *Controlled Release* **2008**, *129*, 228.
22. Xing, N.; Chen, Y.; Mitchell, S. H.; Young, C. Y. *Carcinogenesis* **2001**, *22*, 409.
23. Fessi, H.; Puisieux, F.; Devissaguet, J. P.; Ammoury, N.; Benita, S. *Int. J. Pharm.* **1989**, *55*, R1.
24. Bilati, U.; Allémann, E.; Doelker, E. *Eur. J. Pharm. Sci.* **2005**, *24*, 67.
25. Devanand, K.; Selser, J. C. *Macromolecules* **1991**, *24*, 5943.
26. d'Acunzo, F.; Le, T. Q.; Kohn, J. *Macromolecules* **2002**, *35*, 9366.
27. Van Butsele, K.; Sibret, P.; Fustin, C. A.; Gohy, J. F.; Passirani, C.; Benoit, J. P.; Jérôme, R.; Jérôme, C. *J. Colloid Interface Sci.* **2009**, *329*, 235.
28. Vangeyte, P.; Leyh, B.; Auvray, L.; Grandjean, J.; Misselyn-Bauduin, A. M.; Jérôme, R. *Langmuir* **2004**, *20*, 9019.
29. Tuominen, J. A.; Seppälä, J. V. *Macromolecules* **2000**, *33*, 3530.
30. Jeong, Y. I.; Cheon, J. B.; Kim, S. H.; Nah, J. W.; Lee, Y. M.; Sung, Y. K.; Akaike, T.; Cho, C. S. J. *Controlled Release* **1998**, *51*, 169.
31. Gref, R.; Minamitake, Y.; Peracchia, M. T.; Trubetskoy, V.; Torchilin, V.; Langer, R. *Science* **1994**, *263*, 1600.
32. Vlad, S.; Oprea, S.; Stanciu, A.; Ciobanu, C.; Bulacovschi, V. *Eur. Polym. J.* **2000**, *36*, 1495.
33. Chatti, S.; Behnken, G.; Langanke, D.; Kricheldorf, H. R. *Macromol. Chem. Phys.* **2006**, *207*, 1474.
34. Pralhad, T.; Rajendrakumar, K. *J. Pharm. Biomed. Anal.* **2004**, *34*, 333.
35. Morokuma, K. *Acc. Chem. Res.* **1977**, *10*, 294.
36. Egan, R. W. *J. Biol. Chem.* **1976**, *251*, 4442.
37. Cambón, A.; Alatorre-Meda, M.; Juárez, J.; Topete, A.; Mistry, D.; Attwood, D.; Barbosa, S.; Taboada, P.; Mosquera, V. *J. Colloid Interface Sci.* **2011**, *361*, 154.